

Note

Hydrothermal synthesis and characterization of a novel 3D open framework structure of mixed valence ethylenediamine–vanadium phosphate: $[\text{C}_2\text{H}_{10}\text{N}_2]\text{[(HV}^{\text{IV}}\text{O}_3)(\text{HV}^{\text{V}}\text{O}_2)(\text{PO}_4)]$

Jian-Xin Chen^{*}, Chun-Xia Wei, Zhi-Chun Zhang, Yuan-Biao Huang, Ting-Yan Lan, Zhong-Shui Li, Wen-Jie Zhang

College of Chemistry and Materials Science, Fujian Normal University, Fuzhou, Fujian 350007, PR China

Received 19 February 2006; received in revised form 9 April 2006; accepted 10 April 2006

Available online 26 April 2006

Abstract

A new three-dimensional open framework structure of mixed valence ethylenediamine–vanadium phosphate $[\text{C}_2\text{H}_{10}\text{N}_2][(\text{HV}^{\text{IV}}\text{O}_3)(\text{HV}^{\text{V}}\text{O}_2)(\text{PO}_4)]$ (**1**), has been synthesized under mild hydrothermal conditions and characterized by elemental analyses, IR, fluorescent spectrum, TG-DTA and single crystal X-ray diffraction. Compound **1** exhibits a novel three-dimensional (3D) vanadium phosphate anion framework composed of vanadium, phosphate, and oxygen atoms through covalent bonds, with the diprotonated ethylenediamine $[\text{NH}_3\text{CH}_2\text{CH}_2\text{NH}_3]^{2+}$ cations residing in the channels along *c*-axis. The organic diprotonated ethylenediamine cations interact with the O atoms in the inorganic network through hydrogen bonds. The electrochemical behavior of **1** has also been studied in detail by cyclic voltammograms, which is very important for practical applications in electrode modification. Furthermore, the strong photoluminescence property of compound **1** is also measured at room temperature.

© 2006 Elsevier B.V. All rights reserved.

Keywords: Hydrothermal synthesis; Mixed valence; Vanadium phosphate; 3D framework; Fluorescent property; TG-DTA; Cyclic voltammogram

1. Introduction

Vanadium phosphate phases have been intensively studied due to the wide diversity of their structural chemistry, a concomitant diversity of electronic and magnetic properties, and because of their potential applications in catalysis, adsorption, ion exchange [1–4], and their versatile intercalation properties [5–7]. An astonishing variety of novel phases arise from the combination of vanadium/phosphate progenitors and small organic molecules [8–15]. Such structural variety arises due to the versatility of vanadium in terms of its variable oxidation state (V^{III} , V^{IV} , V^{V}) and

coordination geometry (tetrahedral, square pyramidal, trigonal bipyramidal, and octahedral), combined with the structure-directing (Templating) effect of the organic moiety, although, as yet, we have little control over such synthesis processes. A large number of vanadium phosphates incorporating organic species such as monoammonium and diammonium cations are known. Depending on the charge, shape, and size of the organic cation, structures with rings/cages, cavities, or layers are formed [16]. Several vanadium phosphates containing diprotonated piperazine (pipz-VPOs) have been previously reported. Examples include layered structures closely related to the structure of $\alpha\text{-VOPO}_4 \cdot 2\text{H}_2\text{O}$ and framework structures with tunnels occupied by diprotonated piperazine cations [11,17–20].

In this paper, we report the synthesis, single-crystal structure, and characterization of the first example of

^{*} Corresponding author. Tel.: +86 591 83448669; fax: +86 591 83465376.

E-mail address: jxchen_1964@163.com (J.-X. Chen).

mixed-valence ethylenediamine–vanadium phosphate compound, $[\text{C}_2\text{H}_{10}\text{N}_2][(\text{HVO}_3)(\text{HVO}_2)(\text{PO}_4)]$. This phase has a crystal structure that is completely different from that of compounds [21–23] reported, and shows strong three-dimensional character and structural similarity to the 2D compound $[(\text{C}_6\text{H}_{16}\text{N}_2)_3(\text{VO})(\text{V}_2\text{O}_4)_2(\text{PO}_4)_4 \cdot 2\text{H}_2\text{O}]$ [24]. Both the title compound and the reported compound have an uniform V–O–V linkage in the structure. But the 2D compound has two kinds of V–O–V chains.

2. Experimental

2.1. Reagents

All analytical grade chemicals and solvents were purchased commercially and used without further purification.

2.2. Measurements

Infrared spectrum was measured on a Nicolet AVATAR 360 FT-IR spectrometer using KBr pellets in the 4000–400 cm^{-1} region. Emission/excitation spectra were recorded on a RF-540 fluorescence spectrophotometer. Elemental analyses were carried out on an EA1112 CHNS elemental analyzer. The thermal gravimetric analysis (TGA) and the differential analysis (DTA) were carried out under N_2 with a Switzerland METTLER TGA/SDTA 851 differential thermal analyzer at a rate of 10 $^\circ\text{C min}^{-1}$ in the range 50–800 $^\circ\text{C}$.

Cyclic voltammogram (CV) was recorded on a 384B polarographic analyzer. A CHI 660 Electrochemical Workstation connected to a Digital-586 personal computer was used for control of the electrochemical measurements and for data collection. A conventional three-electrode system was used. The working electrode was a modified carbon paste electrode (CPE). An Ag/AgCl (saturated KCl) electrode was used as a reference electrode and a Pt gauze as a counter electrode. All potentials were measured and reported versus the Ag/AgCl electrode.

Structural measurement for **1** was performed on Rigaku R-Axis RAPID Weissenberg IP diffractometer equipped with a graphite-monochromatized Mo $\text{K}\alpha$ radiation ($\lambda = 0.71073 \text{ \AA}$). Data were collected at 293 K. Lorentz-polarization corrections and empirical absorption correction were applied to the data. The structure was solved by direct methods with SHELXS-97 [25a] and refined by full-matrix least-squares calculations with SHELXL-97 [25b]. All non-hydrogen atoms were refined with anisotropic thermal parameters, and most hydrogen atoms were located in the calculated positions. All calculations were performed on a Pentium IV computer. A summary of the crystallographic data and structural determination for compound **1** is listed in Table 1. Selected bond lengths are provided in Table 2. Atomic coordinates and equivalent isotropic displacement parameters are given in Table S1 (ESI) and Table S2 (ESI) for **1**, respectively.

Table 1
Crystallographic data for **1**

Compound	1
Formula	$\text{C}_2\text{H}_{12}\text{N}_2\text{O}_9\text{PV}_2$
Formula weight	340.99
Crystal system	orthorhombic
Space group	$P2(1)2(1)2(1)$
a (\AA)	8.3176(3)
b (\AA)	9.1539(3)
c (\AA)	12.6302(5)
α ($^\circ$)	90
β ($^\circ$)	90
γ ($^\circ$)	90
V (\AA^3)	961.64(6)
Z	4
D_{calc} (Mg m^{-3})	2.355
Crystal size (mm)	$0.51 \times 0.32 \times 0.31$
μ (mm^{-1})	2.151
$F(000)$	684
$\theta_{\text{max}}, \theta_{\text{min}}$ ($^\circ$)	27.50, 2.75
Index range	
h	$0 \rightarrow 10$
k	$0 \rightarrow 11$
l	$0 \rightarrow 16$
R_{int}	0.0270
No. of independent reflections	1285
No. of observed reflections	1270
No. of variables	152
R	0.0241
wR	0.0832
Goodness-of-fit	1.016
Largest difference in peak ^a (hole) (e \AA^{-3})	0.647 (–0.468)
Δ/σ	0.000, 0.000

$$R = \frac{\sum |F_o| - |F_c|}{\sum |F_o|}, wR = \left\{ \frac{\sum [w(F_o^2 - F_c^2)^2]}{\sum w(F_o^2)^2} \right\}^{1/2}$$

^a Largest peak (hole) in difference Fourier map.

2.3. Preparation of the complex

A mixture of $\text{NH}_2\text{CH}_2\text{CH}_2\text{NH}_2$ ($\text{C}_2\text{H}_8\text{N}_2$, ethylenediamine, 0.75 mmol), V_2O_5 (0.0455 g, 0.25 mmol), P_2O_5 (0.0355 g, 0.25 mmol), $\text{Cd}(\text{OAc})_2$ (0.0576 g, 0.25 mmol), HF (0.1 mL), and 12 mL H_2O was sealed in a 23 mL Teflon-lined stainless steel autoclave with about 60% filling. The pH value was up to about 3 through the addition of a 6 M HCl solution. The resulting mixture was heated at a rate of ca. 100 $^\circ\text{C h}^{-1}$ to 170 $^\circ\text{C}$ and held at this temperature for 2 days. Subsequently the autoclave was cooled at a rate of ca. 3 $^\circ\text{C h}^{-1}$ to 140 $^\circ\text{C}$ and held at this temperature for 3 days. Finally, it was cooled at a rate of ca. 4 $^\circ\text{C h}^{-1}$ to room temperature. The resulting prism black crystals were filtered off and washed with water, then dried at ambient temperature. Yield: 0.0341 g (20% based on V). Anal. Calc. for $\text{C}_2\text{H}_{12}\text{N}_2\text{O}_9\text{PV}_2$ (**1**): C, 7.04; H, 3.52; N, 8.21; P, 9.09; V, 29.90. Found: C, 7.06; H, 3.50; N, 8.26; P, 9.05; V, 29.92%. In this synthesis, without the incorporation of the metal cations Cd^{2+} , the role of this metallic cation is unknown but not unprecedented; for example, a barium vanadium(IV) phosphate hydrate, $\text{Ba}_2\text{VO}(\text{PO}_4) \cdot \text{H}_2\text{O}$ [26], required the presence of Zn^{2+} to form, although no zinc was incorporated in the majority product.

Table 2
Selected bond lengths (Å) and bond angles (°) for **1**

V(1)—O(1)	1.605(3)	V(1)—O(2)	1.709(3)	V(1)—O(4)	1.930(3)
V(1)—O(8)	1.944(2)	V(1)—O(3)#1	1.978(3)	V(2)—O(5)	1.588(3)
V(2)—O(9)	1.922(3)	V(2)—O(2)#2	1.950(3)	V(2)—O(6)#3	1.974(3)
V(2)—O(7)	2.003(3)	V(2)—O(8)	2.311(3)	P(1)—O(6)	1.527(3)
P(1)—O(7)	1.533(3)	P(1)—O(4)	1.539(3)	P(1)—O(3)	1.552(3)
O(1)—V(1)—O(4)	101.78(15)	O(2)—V(1)—O(4)	91.42(13)	O(1)—V(1)—O(8)	106.85(14)
O(2)—V(1)—O(3)#1	89.92(13)	O(4)—V(1)—O(3)#1	156.97(15)	O(8)—V(1)—O(3)#1	80.67(11)
O(5)—V(2)—O(9)	97.60(16)	O(5)—V(2)—O(2)#2	102.47(17)	O(1)—V(1)—O(2)	106.20(16)
O(5)—V(2)—O(6)#3	101.34(16)	O(9)—V(2)—O(6)#3	90.98(13)	O(2)#2—V(2)—O(6)#3	87.26(13)
O(2)#2—V(2)—O(8)	81.42(12)	O(6)#3—V(2)—O(8)	84.36(11)	O(7)—V(2)—O(8)	78.88(10)
O(6)—P(1)—O(7)	108.21(17)	O(6)—P(1)—O(4)	110.51(17)	O(7)—P(1)—O(4)	109.59(16)
O(6)—P(1)—O(3)	107.80(17)	O(7)—P(1)—O(3)	111.32(15)	O(4)—P(1)—O(3)	109.39(17)

Symmetry transformations used to generate equivalent atoms.

#1 $x - 1/2, -y + 3/2, -z$; #2 $x + 1/2, -y + 3/2, -z$; #3 $-x + 1/2, -y + 1, z - 1/2$.

3. Results and discussion

3.1. Structure description

Selected bond distances and angles for **1** are listed in Table 2. The structure of **1** contains [(HVO₃)(HVO₂)(PO₄)]²⁻ framework separated by diprotonated ethylenediamine cations. A fragment of the molecular structure showing the atom-labeling scheme is shown in Fig. 1, and the unit cell packing is illustrated in Fig. 2. One crystallographically distinct V(1)O₅ tetragonal pyramids, V(2)O₆ octahedron, and PO₄ tetrahedron are connected by sharing oxygen atoms. The V(1)O₅ tetragonal pyramid has two short V=O bonds (V(1)—O(1), 1.605(3) Å; V(1)—O(2), 1.709(3) Å) and three intermediate V—O bonds with the distances of 1.930(3)–1.978(3) Å. The longer bond distances are coordinated to neighboring P(1) center and V(2) center (see Fig. 1). The V(2)O₆ octahedron has one short bond V(2)=O(5) (1.588(3) Å), One much longer bond

V(2)—O(8) (2.311(3) Å, *trans* to V(2)=O(5)), and the other four V—O bonds with the distances of 1.922(3)–2.003(3) Å. The O—V(1)—O angles are in the range of 80.67(11)–156.97(15)° and O—V(2)—O in 78.40(11)–173.17(14)°. Four P—O bonds of PO₄ are in the range 1.527(3)–1.552(3) Å. All P—O bonds are connected to four vanadium atoms via four μ₂-oxygen atoms (O(3), O(4), O(6) and O(7)), and O—P—O angles are in the range of 107.80(17)–111.32(15)°. Bond valence sum (BVS) calculations [27] yielded values of 4.762 for V(1) and 4.418 for V(2), which are close to 5 and 4, respectively. Magnetic measurement supported the BVS calculations suggesting the existence of a *d*¹ vanadium (IV) atom and a *d*⁰ vanadium (V) atom. BVS(P) in the PO₄ group is 4.786. BVS calculations indicate that all oxygen atoms have values close to 2 except O(8) and O(9), which are 0.724 and 0.937, respectively. The valence sum in the case of O(8) and O(9) from V atoms are satisfied by partially protonating. So the position of H in (HVO₃)(HVO₂) groups are chemically reasonable. According to the consideration of the charge balance and the weak acidic environment of synthesis system, the di-protonated ethylenediamine molecule [C₂H₁₀N₂]²⁺ and [(HVO₃)(HVO₂)(PO₄)]²⁻ are co-exist in the compound **1**, which is a common feature in many reported literatures [28,29]. These cations and polyoxoanion are contacted with each other through electrostatic interactions and weak hydrogen bonds.

As shown in Fig. 2, each V(2)O₆ octahedron shares corners with one PO₄ tetrahedron to form the infinite one-dimensional linear chain structure along *c*-axis. And the neighboring one-dimensional chains, are linked together in the corner sharing manner through adjacent V(1)O₅ tetragonal pyramids, giving rise to the formation of two-dimensional layers parallel to the *ac*-plane (Fig. 2). These two-dimensional layers stack along *b*-axis are linked together by bridging V(1)O₅ tetragonal pyramids to further extend the structure to a three-dimensional framework (Fig. 3a). This organization leads to the formation of channels in two directions: along the *c*-axis 1D channels can be observed with dimensions of about 6.1465(11) ×

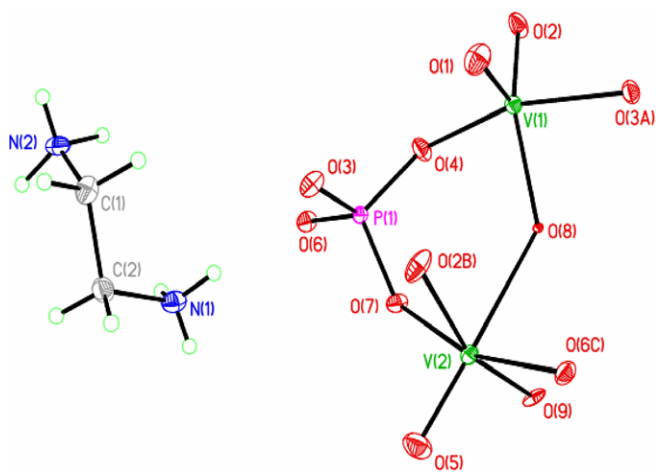


Fig. 1. View of a fragment of the molecular structure of complex **1**. Thermal ellipsoids are shown with 50% probability. Symmetry operation code: A $x - 1/2, -y + 3/2, -z$; B $x + 1/2, -y + 3/2, -z$; C $-x + 1/2, -y + 1, z - 1/2$.

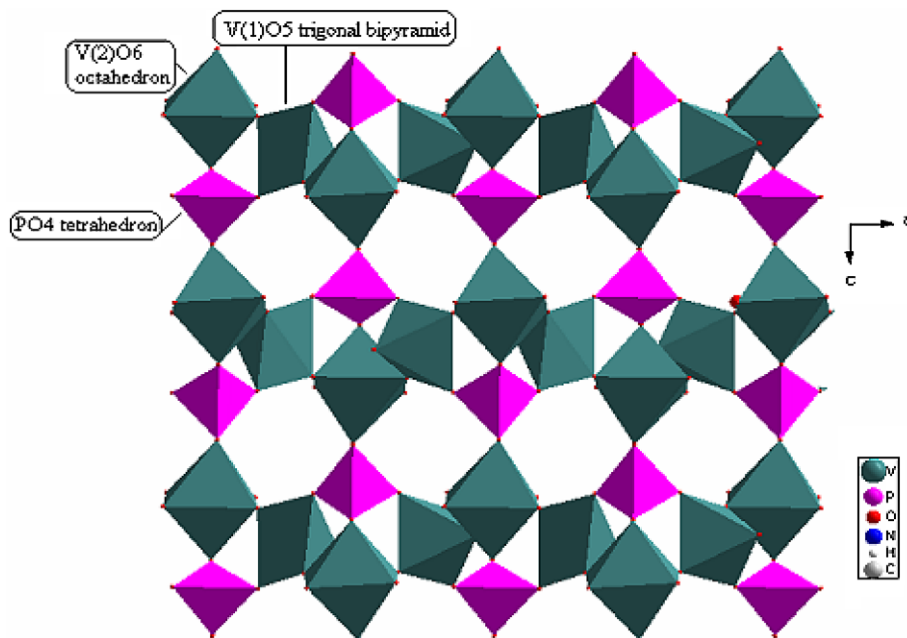


Fig. 2. Polyhedral representation of the 2D network in **1** and diprotonated ethylenediamines omitted.

5.9968(11) Å (based on nucleus separation, Fig. 3b). The second channels are shown in Fig. 2, which are comprised of tetranuclear metallic cores {V₄} with the diameter of ca. 4 Å along the *b*-axis. As observed in related materials [30–34], this type of arrangement leads to a cavity, tunnel-like, cage-like or window-like. And crystal packing of **1** along the *a*-axis can be seen from Fig. 4. Free diprotonated ethylenediamines are located in these channels along the *c* axis. The organic diprotonated ethylenediamines cations interact with the O atoms in the inorganic network through H-bonds with the N...O separation in the range of 2.684–3.136 Å (Fig. 5). The typical hydrogen bonds are N2...O9, N2...O1, N1...O9, N1...O8, N1...O3 (shown in Table 3). It is believed that the extensive hydrogen-bonding interactions between guest molecules and the framework play an important role in stabilizing the 3D structure.

The structure of **1** with the chiral space group *P*2₁2₁2₁ is somewhat curious and unanticipated. There are a number of unusual features associated with this unit in **1**, when compared to those reported compounds [24,33,35], the vanadium sites are tetragonal pyramid and octahedron rather than tetrahedral or trigonal bipyramidal. The phosphate tetrahedral engage in corner-sharing to four vanadium sites. The corner-sharing linkage between V(1)O₅ tetragonal pyramids, V(2)O₆ distorted octahedron and PO₄ tetrahedron are crucial in the formation of the three-dimensional frameworks. There are open channels along *c*-direction and *b*-direction in the compound.

3.2. IR spectrum

The infrared spectrum of **1** is shown in Fig. 6. Prominent bands attributable to N–H, P–O, V=O, and V–O vibrational modes may be assigned by comparison with IR data

for related structures [33,36,37]. Bands in the 3100–3450 cm⁻¹ region can be attributed to N–H stretching, while those in the 1500–1700 cm⁻¹ are due to protonated ethylenediamine ending modes. The peaks at 1099 and 1042 cm⁻¹ are assigned to P–O stretch. And the strong bands at 970 cm⁻¹ is due to the stretching vibrations of the terminal V=O bonds, and the bands at 819 cm⁻¹ is attributable to the stretching vibrations of V–O–V bonds. The peaks round 631, 596, and 470 cm⁻¹ are probably ascribed to the vibrations of V–O or V–O–P bonds. The IR confirmed the presence of diprotonated ethylenediamines cations and [(HVO₃)(HVO₂)(PO₄)]²⁻ anions in the structure.

3.3. Fluorescent property

The fluorescent spectrum of the solid state of the compound (**1**) at room temperature shows that maximum emission peaks occurred at ca. 435 nm upon excitation at ca. 375 nm (Fig. 7). The emission spectrum of compound **1** may be attributed to an intra-ligand emission state instead of ligand-to-metal charge transfer (LMCT) in nature. The results indicated that compound (**1**) is potential fluorescent-emitted material.

3.4. Thermal gravimetric analysis

Thermogravimetric measurements of compound **1** show that compound **1** is stable below 290 °C, and the diprotonated ethylenediamine molecules released in the region 290–430 °C with a weight loss of 17.81% (calc. 18.18%). In the range of 430–800 °C the step of weight loss of 52.74% is corresponding to the decomposition of vanadium phosphate. A noteworthy finding is that there is still weight loss above 800 °C.

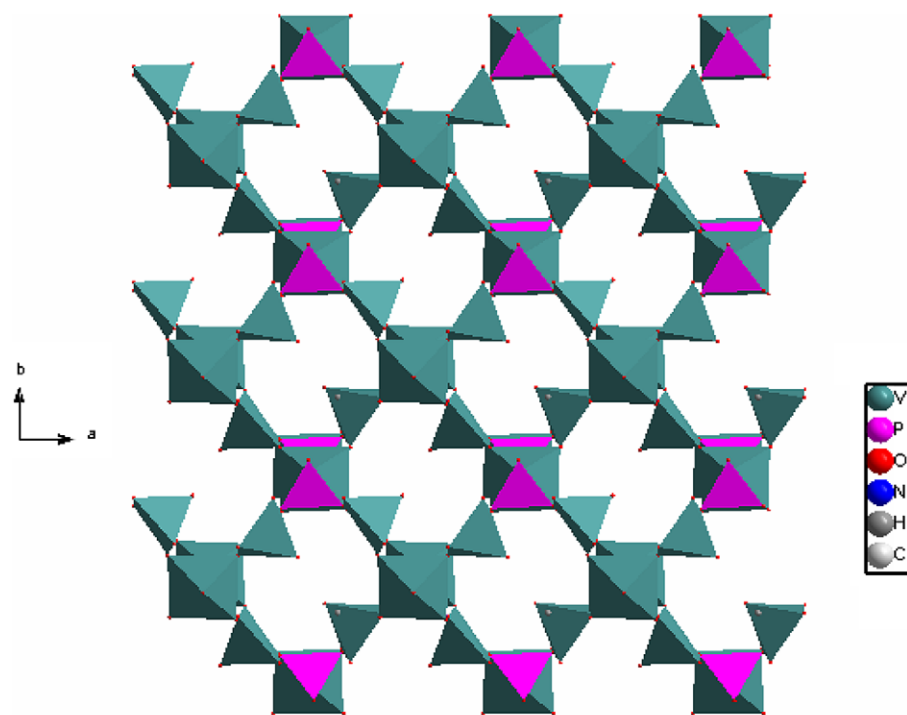
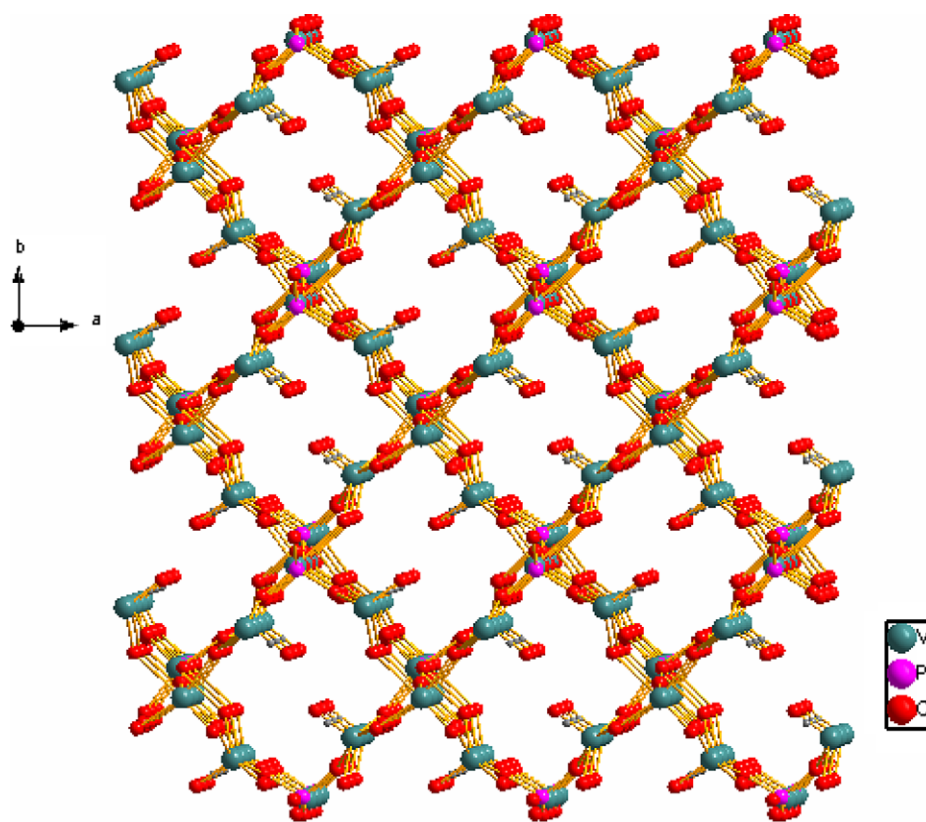


Fig. 3. (a) View of crystal packing of **1** along the *c*-axis showing square channels. (b) Polyhedral diagram of **1** along the *c*-axis showing the 1D channels. (All diprotonated ethylenediamine molecules are omitted for clarity.)

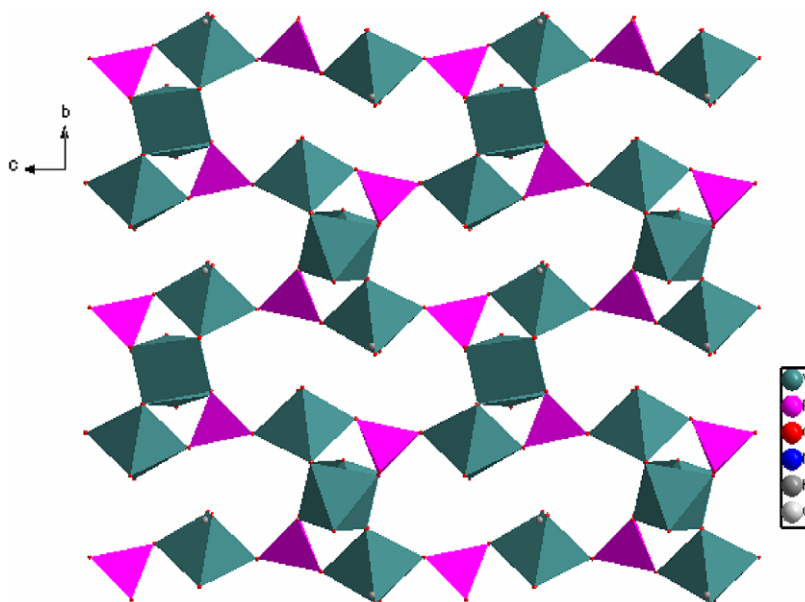


Fig. 4. View of crystal packing of **1** along the *a*-axis with diprotonated ethylenediamines omitted.

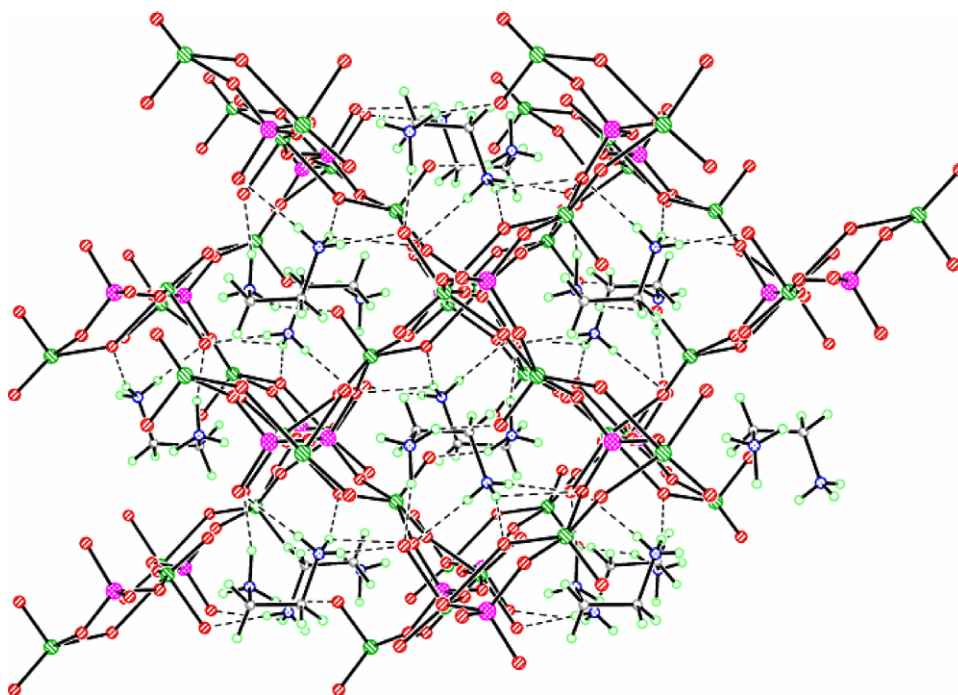


Fig. 5. Detail of the $[\text{C}_2\text{H}_{10}\text{N}_2][(\text{HVO}_3)(\text{HVO}_2)(\text{PO}_4)]$ structure showing the hydrogen bonding of the diprotonated ethylenediamines cations.

3.5. Voltammetric behavior

3.5.1. Preparation of 1-CPE

Compound **1** nanoparticle modified CPE (**1-CPE**) was fabricated as follows: 0.1607 g graphite powder and 0.046 g compound **1** were mixed and ground together by agate mortar and pestle to achieve an even, dry mixture; to the mixture 0.10 mL paraffin oil was added and stirred with a glass rod; then the mixture was used to paste on a 6 mm diameter carbon bar, and the surface was pressed tightly

by a clean knife. Electrical contact was established through carbon bar electrode.

3.5.2. Voltammetric behavior of 1-CPE in aqueous electrolyte

Fig. 8 presents the cyclic voltammetric behavior for **1-CPE** in 1 M H_2SO_4 aqueous solution at scan 20 mV s^{-1} . It can be seen from Fig. 8 that in the potential range +1600 to 0 mV, two reversible redox peaks appear. The mean peak potentials $E_{1/2} = (E_{\text{pa}} + E_{\text{pc}})/2$ are 834 mV (**I**),

Table 3
Hydrogen-bonding geometry (Å, °)

D—H...A	D—H	H...A	D...A	∠(DHA)
N2—H4N...O1#1	0.92	2.07	2.930(5)	154.7
N2—H5N...O9#2	1.02	1.71	2.684(5)	159.1
N1—H1N...O9#3	0.73	2.00	2.727(4)	171.9
N1—H2N...O8#2	0.91	1.94	2.816(4)	162.1
N1—H2N...O3#4	0.91	2.52	3.136(5)	125.2
N1—H3N...O3	0.84	2.18	3.023(5)	173.6

Symmetry codes: #1 $-x+1, y-1/2, -z+1/2$; #2 $-x+1/2, -y+1, z+1/2$; #3 $x+1/2, -y+1/2, -z$; #4 $-x+1, y-1/2, -z+1/2$.

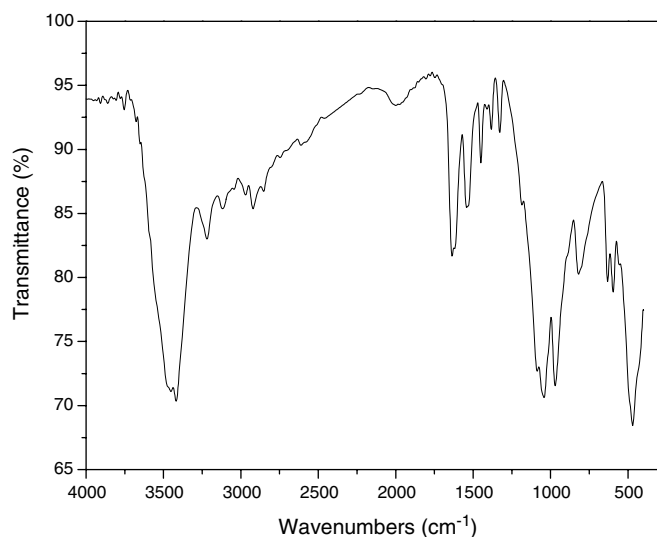


Fig. 6. Infrared spectrum for the title compound.

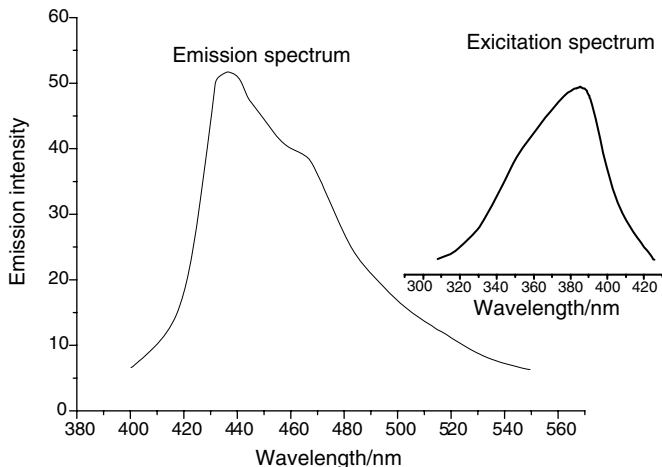


Fig. 7. Solid-state emission spectrum of the compound **1** at room temperature.

and 258 mV (II), respectively. Redox peaks II–II' correspond to one-electron process and I–I' correspond to two-electron process. Two reduction peaks potentials E_{pc} are 757 and 219 mV, respectively, while the two oxidation peaks appear at 911 and 296 mV, respectively.

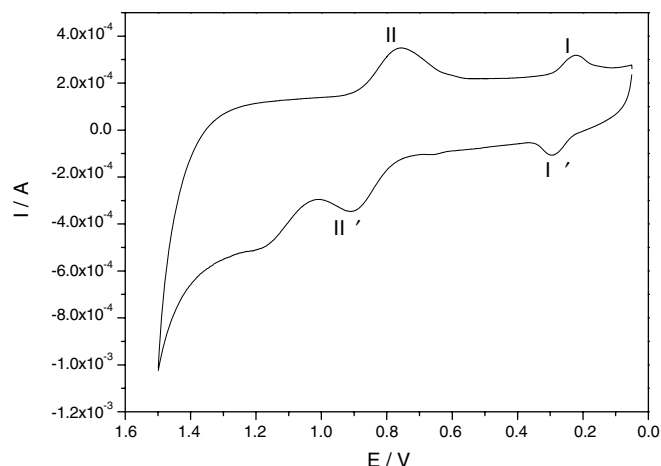


Fig. 8. Voltammogram of the **1-CPE** in 1 M H_2SO_4 at a scan rate of 20 mV s^{-1} .

The oxidation peak present in 1.1 V in Fig. 8 voltammogram of **1-CPE** in aqueous electrolyte contributes to the exorbitant potential, resulting in that water is oxidized to give rise to O_2 . It may be that the reduction peak potential and the II potential overlap, so there is no corresponding reduction peak matching to this oxidation peak.

When the scan rate was varied from 20 to 200 mV s^{-1} , the peak potentials changed gradually: the cathodic peak potentials shifted toward the negative direction and the corresponding anodic peak potentials to the positive direction with increasing scan rates. When scan rates were lower than 120 mV s^{-1} , the peak currents were proportional to the scan rate (see Fig. 9), which indicates that the redox process of **1-CPE** is surface-controlled, ideally reversible, and the exchanging rate of electrons is fast; however, when scan rates were higher than 120 mV s^{-1} , the peak currents were proportional to the square root of the scan rate, which indicates that the redox process of **1-CPE** is diffusion-controlled.

When cyclic scan was performed in the same potential range for many times at 50 mV s^{-1} , the cyclic voltammogram of the **1-CPE** was unchanged. Namely, after one-cycle sweeping and returning to the complete oxidation form, the compound **1** in CPE makes no change, although the reduction and oxidation process are not symmetric, which is similar to what Dong et al. have reported [38]. Therefore, the sweep was confined to the two waves. The compound **1** is active center for electrochemical redox in the solutions. And the **1-CPE** was stored at room temperature ($20\text{--}25 \text{ }^\circ\text{C}$) for at least two weeks, the current response remained almost unchanged, it shows remarkable stability. The remarkable stability for **1-CPE** should be ascribed to the insolubility of the inorganic–organic hybrid material. The extensive hydrogen bonding and packing interactions existed in crystal structure may serve the insolubility of **1** in aqueous solution. Many studies have shown that reduced materials are capable of delivering the electrons to other species, thus serving as powerful electron

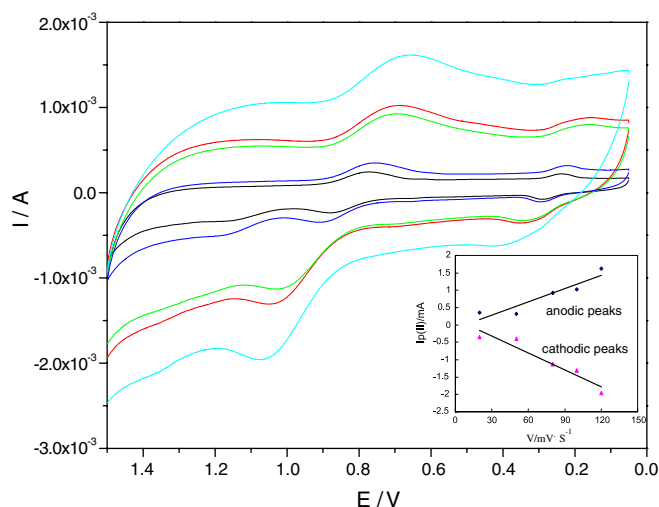


Fig. 9. The cyclic voltammograms of 1-CPE in 1 M H_2SO_4 aqueous solution at different scan rates (from inner to outer: 20, 50, 80, 100 and 120 mV s^{-1}). The inset shows plots of the anodic and cathodic peak II–II' current against scan rates.

reservoirs for multi-electron reductions. This property can be exploited extensively in electrocatalytic reductions.

4. Conclusions

In summary, a novel mixed valence vanadium phosphate **1** has been obtained as X-ray quality single crystals under the hydrothermal conditions. It is an interesting vanadium phosphate, in particular, the chiral space group $P2_12_12_1$ of this compound is rather uncommon in open-framework metal phosphates. The crystal structure of the compound contain PO_4 tetrahedron, $\text{V}(1)\text{O}_5$ tetragonal pyramids, and $\text{V}(2)\text{O}_6$ distorted octahedron, where the corner-sharing linkage between $\text{V}(1)\text{O}_5$ tetragonal pyramids, $\text{V}(2)\text{O}_6$ distorted octahedron and PO_4 tetrahedron are crucial in the formation of the three-dimensional frameworks. There are open channels along the *b*-direction and *c*-direction in the compound, where the counter cations are located along *c*-direction. And the organic diprotonated ethylenediamines cations interact with the O atoms in the inorganic network through hydrogen bonds. Vanadium phosphates continue to attract attention as cavity and open framework materials potentially manifesting porous properties [39–41]. The search for new materials of this family has now focused on structural modification and design of oxo-vanadium phosphates through the introduction of organic components as charge-compensating, space-filling and overall structure-directing cations. So we are continuing our investigations into vanadium/phosphate phases templated by small organic entities. Furthermore, Thermogravimetric measurements of compound **1** show that compound **1** is stable below 290 °C, and the strong photoluminescence property of compound **1** may make it excellent candidates for potential photoactive materials. And the electrochemical behavior of **1** shows remarkable stability and reduction. So compound **1** can be applied as

catalysts for the reduction of hydrogen, peroxide and nitrite, and so on.

Acknowledgments

The authors are thankful for the financial supports from the Natural Science Foundation of Fujian Province, China (E0310016) and the Education Commission Foundation of Fujian Province, China (JB05309).

Appendix A. Supplementary data

Crystallographic data for the compound **1** has been deposited at the Cambridge Crystallographic Data Center as supplementary publications (CCDC-290728). These data can be obtained free of charge at www.ccdc.cam.ac.uk/conts/retrieving.html [or from the Cambridge Crystallographic Data Center, 12, Union Road, Cambridge CB2 1EZ, UK; fax: +44 1223/336 033; mail to: deposit@ccdc.cam.ac.uk.] Supplementary data associated with this article can be found, in the online version, at doi:10.1016/j.ica.2006.04.025.

References

- [1] J.W. Johnson, D.C. Johnston, A.J. Jacobson, J.R. Brody, *J. Am. Chem. Soc.* 106 (1984) 8123.
- [2] D. Beltran-Porter, P. Amoros, R. Ibanez, E. Martinez, A. Beltran-Porter, A. Le Bail, G. Férey, G. Villeneuve, *Solid State Ionics* 32–33 (1989) 57.
- [3] P. Amoros, A. Beltran, D. Beltran, *J. Alloys Compd.* 188 (1992) 123.
- [4] K.-H. Lii, *J. Chin. Chem. Soc.* 39 (1992) 569.
- [5] S. Boudin, A. Guesdon, A. Leclaire, M.-M. Borel, *Int. J. Inorg. Mater.* 2 (2000) 561.
- [6] M. Eddaoudi, D.B. Moler, H. Li, B. Chen, T.M. Reineke, M. O'Keeffe, O.M. Yaghi, *Acc. Chem. Res.* 34 (2001) 319, and references therein.
- [7] G. Férey, *Chem. Mater.* 13 (2001) 3084, and references therein.
- [8] V. Soghomonian, Q. Chen, R.C. Haushalter, J. Zubieta, C.J. O'Connor, *Science* 259 (1993) 1596.
- [9] V. Soghomonian, Q. Chen, R.C. Haushalter, J. Zubieta, *Angew. Chem. Int., Ed. Engl.* 32 (1993) 610.
- [10] V. Soghomonian, Q. Chen, R.C. Haushalter, J. Zubieta, *Chem. Mater.* 5 (1993) 1690.
- [11] V. Soghomonian, R.C. Haushalter, Q. Chen, J. Zubieta, *Inorg. Chem.* 33 (1994) 1700.
- [12] M.L. Khan, L.M. Meyer, R.C. Haushalter, A.L. Schweizer, J. Zubieta, J.L. Dye, *Chem. Mater.* 8 (1996) 43.
- [13] G. Bonavia, R.C. Haushalter, C.J. O'Connor, J. Zubieta, *Inorg. Chem.* 35 (1996) 5603.
- [14] T. Loiseau, G. Férey, *J. Solid State Chem.* 111 (1994) 416.
- [15] W.T.A. Harrison, K. Hsu, A.J. Jacobson, *Chem. Mater.* 7 (1995) 2004.
- [16] F. Bontchev, J. Do, A.J. Jacobson, *Angew. Chem., Int. Ed.* 38 (1999) 1937.
- [17] D. Riou, G. Férey, *Eur. J. Solid State Inorg. Chem.* 31 (1994) 31.
- [18] V. Soghomonian, Q. Chen, Y. Zhang, R.C. Haushalter, C.J. O'Connor, C. Tao, J. Zubieta, *Inorg. Chem.* 34 (1995) 3509.
- [19] V. Soghomonian, R.C. Haushalter, J. Zubieta, C.J. O'Connor, *Inorg. Chem.* 35 (1996) 2830.
- [20] X. Bu, P. Feng, G.D. Stucky, *J. Chem. Soc., Chem. Commun.* (1995) 1337.

- [21] L.M. Mokry, J. Thompson, M.R. Bond, T. Otieno, M. Mohan, C.J. Carrano, *Inorg. Chem.* 33 (1994) 2705.
- [22] M. Schindler, W. Joswig, W.H. Baur, *J. Solid State Chem.* 145 (1999) 15.
- [23] J. Do, R.P. Bontchev, A.J. Jacobson, *J. Solid State Chem.* 154 (2000) 514.
- [24] Y. Cui, J. Sun, H. Meng, G. Li, C. Chen, L. Liu, X. Yuan, W. Pang, *Inorg. Chem. Commun.* 8 (2005) 759.
- [25] (a) G.M. Sheldrick, *SHELXS-97*, Program for X-ray Crystal Structure Solution, University of Göttingen, Göttingen, Germany, 1997;
(b) G.M. Sheldrick, *SHELXL-97*, Program for X-ray Crystal Structure Refinement, University of Göttingen, Göttingen, Germany, 1997.
- [26] W.T.S. Harrison, S.C. Lim, J.T. Vaughey, A.J. Jacobson, D.P. Goshorn, J.W.J. Johnson, *Solid State Chem.* 113 (1994) 444.
- [27] T.B. Zunic, I.J. Vickovic, *Appl. Crystallogr.* 29 (1996) 305.
- [28] I.D. Williams, M.M. Wu, H.H.-Y. Sung, X.X. Zhang, J.H. Yu, *Chem. Commun.* (1998) 2463.
- [29] L. Xu, Y.Q. Sun, E.B. Wang, *J. Solid State Chem.* 146 (1999) 533.
- [30] M.-L. Tong, B.-H. Ye, J.-W. Cai, X.-M. Chen, S.W. Ng, *Inorg. Chem.* 37 (1998) 2645.
- [31] S. Kawata, S. Kitagawa, M. Kondo, I. Furuchi, M. Munakata, *Angew. Chem., Int. Ed. Engl.* 33 (1994) 1759.
- [32] Y. Lu, Y. Li, E.B. Wang, J. Lu, L. Xu, R. Clérac, *Eur. J. Inorg. Chem.* (2005) 1239.
- [33] B. Gao, S. Liu, L. Xie, X.H. Wang, C. Zhang, C. Sun, N. Hu, H. Jia, *J. Solid State Chem.* 178 (2005) 1825.
- [34] H.Y. An, D.G. Xiao, E.B. Wang, Y.G. Li, X.L. Wang, L. Xu, *Eur. J. Inorg. Chem.* (2005) 854.
- [35] Robert C. Finn, J. Zubieta, *J. Chem. Soc., Dalton Trans.* (2002) 856.
- [36] Z. Biresak, W.T.A. Harrison, *Inorg. Chem.* 37 (1998) 3204.
- [37] J. Do, R.P. Bontchev, A.J. Jacobson, *J. Solid State Chem.* 154 (2000) 514.
- [38] M. Liu, S. Dong, *Electrochem. Acta* 40 (1995) 197.
- [39] C.N.R. Rao, S. Natarajan, S. Neeraj, *J. Am. Chem. Soc.* 122 (2000) 2810, and references therein.
- [40] S. Natarajan, S. Neeraj, A. Choudhury, C.N.R. Rao, *Inorg. Chem.* 39 (2000) 142.
- [41] K.-H. Lii, Y.-F. Huang, V. Zima, C.-Y. Huang, H.-M. Lin, Y.-C. Jiang, F.-L. Liao, S.-L. Wang, *Chem. Mater.* 10 (1998) 2599, and references therein.